Source continuity and boundary discontinuity considerations in Bayesian image processing

Z. Liang and H. Hart
Department of Nuclear Medicine, Montefiore Medical Center, Bronx, New York 10467; and Department of Physics, City College of New York, New York, New York, 10031

(Received 30 September 1987; accepted for publication 24 May 1988)

This paper extends the Bayesian image processing (BIP) formalism by considering the effect of simple source continuity and boundary discontinuity and *a priori* information in estimating an optimal source distribution from observed data. The *a priori* source information is formulated in terms of probability density functions of source element strengths and spatial correlations. The estimation is carried out iteratively by a BIP algorithm derived by applying the expectation maximization technique to the *a priori* source probability density functions and assuming the data obey Poisson statistics. The suppression of boundary oscillations and enhancement of overall image are demonstrated for computer generated ideal and Poisson randomized data.

I. INTRODUCTION

The importance of identifying object boundaries in the source field in image processing is well known.[1,2] Most image processing algorithms that improve image resolution produce spurious oscillations (Gibbs phenomenon) when applied to boundaries. Suppression of such artifacts has made progress using filtering and regularizing techniques.[3–5] The possibility of using *a priori* source information to optimize image processing in general has been proposed in rather global terms.[6,7] We have proposed a Bayesian image processing (BIP) formalism which focuses on individual source element (voxel) probability distribution.[8–13] This latter Bayesian approach has now been applied to treat boundary oscillations. A BIP algorithm has been derived which provides the maximum *a posteriori* result, subject to boundary discontinuity and otherwise nearby source element continuity constraints. The suppression of boundary oscillations while preserving boundary discontinuities is demonstrated by applying the algorithm to computer generated ideal and Poisson randomized data.

II. BIP ALGORITHM

The *a priori* source information of nearby source element continuity and boundary discontinuity can be formulated, in terms of a probability density function $P(\Phi)$, as the following:

$$P(\Phi)=\prod_{j}^{J}\left[C_b\exp\left(-\frac{(\phi_j-\phi_b^e)^2}{2\sigma_b^2}\right)+\sum_{s,s'}^{K}C_s\exp\left(-\frac{(\phi_j-\phi_s^e)^2}{2\sigma_s^2}-\frac{(\phi_{j\pm1}-\phi_{s'}^e)^2}{2\sigma_{s'}^2}\right)\right], \tag{1}$$

where J is the number of voxels, K the number of gray levels above background, and ϕ_j the gray level of voxel j; $\{\phi_s^e\}$ are the distinct estimated gray levels above the estimated background level ϕ_b^e and $\{\phi_{s'}^e \approx \phi_s^e\}$ reflect the nearby source element continuity condition, with or without a limited amount of deviation from ϕ_s^e, σ_b, σ_s, and $\sigma_{s'} \approx \sigma_s$ reflect the variations of gray levels $\{\phi_j\} = \Phi$ around the estimated gray levels $\{\phi_l^e\}$, $l = b,s$, respectively; C_b and $\{C_s\}$ are constants reflecting the relative anticipated frequency of voxels in the ranges about ϕ_b^e and $\{\phi_s^e\}$. Note that the first term $C_b \exp[-(\phi_j-\phi_b^e)^2/2\sigma_b^2]$ reflects the elevated probability for voxel values in the neighborhood of the anticipated background level ϕ_b^e. The summation terms provide significant probabilities for alternative voxel values in the neighborhood of $\phi_j \approx \phi_s^e \neq \phi_b^e$ whenever the adjacent voxels $\phi_{j\pm1}$ have values not too different from $\phi_j \approx \phi_s^e$ (i.e., $\phi_{j\pm1} \approx \phi_{s'}^e$ where $\phi_{s'}^e \approx \phi_s^e$.) The $P(\Phi)$ chosen, therefore reduces the probability of spiky, randomly discontinuous source distributions.

The *a posteriori* probability density function $P(\Phi|Y)$ is given by Bayes' Law:

$$P(\Phi|Y)=P(Y|\Phi)P(\Phi)/P(Y), \tag{2}$$

where the likelihood probability density function $P(Y|\Phi)$ reflects the statistical nature of measured data Y and the data probability density function $P(Y)$ is not related to the maximal value of $P(\Phi|Y)$ and so will be omitted. If there is no *a priori* source information available, $P(\Phi)$ can be assumed as constant, implying that all possible source values are equally likely, then maximizing the *a posteriori* probability function results in the same solution as maximum likelihood.[14–16]

For each data element obeying Poisson statistics with all of them statistically uncorrelated, the conditional probability function $P(Y|\Phi)$ has the form:

$$P(Y|\Phi)=\prod_{i}^{I}\exp\left(-\sum_{j}R_{ij}\phi_j\right)\left(\sum_{j}R_{ij}\phi_j\right)^{Y_i}/Y_i!, \tag{3}$$

where I is the number of data elements, R_{ij} the probability of photons emitted at voxel j and contributing to element Y_i, and $\Sigma_j R_{ij}\phi_j$ the mean of random variable Y_i.[15,16]

In nuclear medical imaging, R_{ij} include the effects of radioisotope decay, tissue attenuation, and scattering and can be determined by scanning a point source (i.e., point spread function).

 0094-2405/88/050754-03$01.20

The optimal solution Φ^* maximizing the *a posteriori* function $P(\Phi|Y)$ is determined by the system of equations of

$$\frac{\partial}{\partial \phi_k} \ln P(\Phi|Y)|_{\Phi=\Phi^*} = 0, \quad k = 1,2,\ldots,J. \tag{4}$$

An iterative algorithm approaching the solution Φ^* is derived, by employing the expectation maximization technique [14–16]:

$$\phi_k^{(n+1)} = \phi_k^{(n)}\left(\sum_i R_{ij}\, Y_i / \sum_j R_{ij}\, \phi_j^{(n)}\right) \Big/ \left(\sum_i R_{ik} + \mu_k^{(n)} Z_k^{(n)}\right), \tag{5}$$

where $\mu_k^{(n)}$ is an adjustable sigmoidal parameter chosen to gradually impose the effect of the *a priori* constraints $P(\Phi)$,

$$\mu_k^{(n)} = \frac{An^\tau}{B + n^\tau} \sum_i R_{ik} \tag{6}$$

with A, B, and τ constant and

$$Z_k^{(n)} = -\frac{\partial}{\partial \phi_k} \ln P(\Phi)|_{\Phi=\Phi^{(n)}+\lambda d^{(n)}} = \frac{U_b \exp(-V_b) + \sum_s \eta_s^{(n)} U_s \exp(-V_s)}{\exp(-V_b) + \sum_s \eta_s^{(n)} \exp(-V_s)}, \tag{7}$$

where $\lambda \approx 1$, $d^{(n)} \approx \Phi^{(n)} - \Phi^{(n-1)}$ are chosen for easy computation of Eq. (5), and

$$U_s = (\phi_k - \phi_s^e)/\sigma_s^2,$$

$$V_s = \frac{(\phi_k - \phi_s^e)^2}{2\sigma_s^2} + \frac{(\phi_{k\pm1} - \phi_{s'}^e)^2}{2\sigma_{s'}^2}; \tag{8}$$

and similarly for U_b and V_b.

The parameter $\eta_s^{(n)}$ is a function of C_b and C_s and is assumed as the following

$$\eta_s^{(n)} = A_s\, n^\kappa/(B_s + n^\kappa) \tag{9}$$

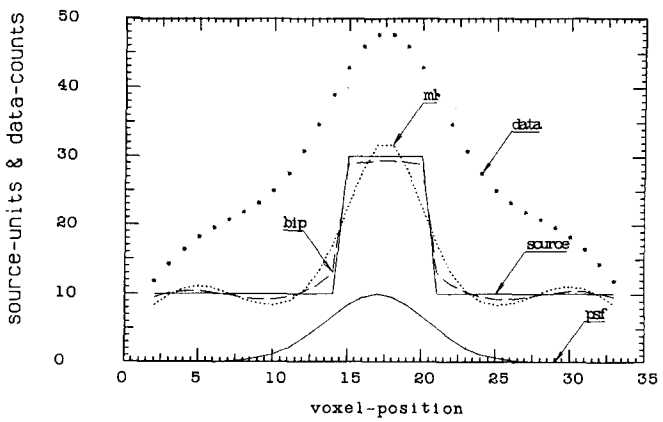

FIG. 1. Comparison of results using BIP (broken line) after 50 iterations and ML (dotted line) after 100 iterations with ideal data (stars) calculated from the convolution of the source distribution and the unnormalized PSF (solid lines). The source units can be expressed in units of radioactivity or in their display equivalent gray levels.

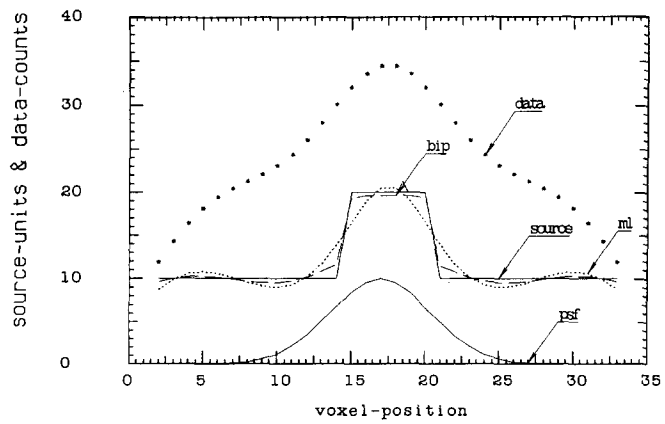

FIG. 2. Comparison of results using BIP (broken line) after 50 iterations and ML (dotted line) after 100 iterations with ideal data (stars), when the source strength above background is halved.

for modifying the relative effect of background, where A_s, B_s, and κ are constants. The general sigmoidal dependence of $\mu_k^{(n)}$ and $\eta_s^{(n)}$ is important for optimal results but the values of the parameters A, B, A_s, B_s, τ, and κ can vary significantly from those used below.

III. SIMULATION RESULTS

Computer simulation results are shown in Figs. 1–5. The source distribution $\{S_j\}$, solid lines shown in Figs. 1–3, is simply chosen as only two gray levels, a background of 10 and a gray level of 20 or 30 source units. The point source spread function (PSF, solid lines in Figs. 1–3) is assumed as the following:

$$R_{ij} \approx \exp[-\ln(2)(i-j)^2/\tau^2], \tag{10}$$

with $T = \text{FWHM}/2 = 4$ voxel units (FWHM: full width at half-maximum). The ideal data (stars in Figs. 1–3) are cal-

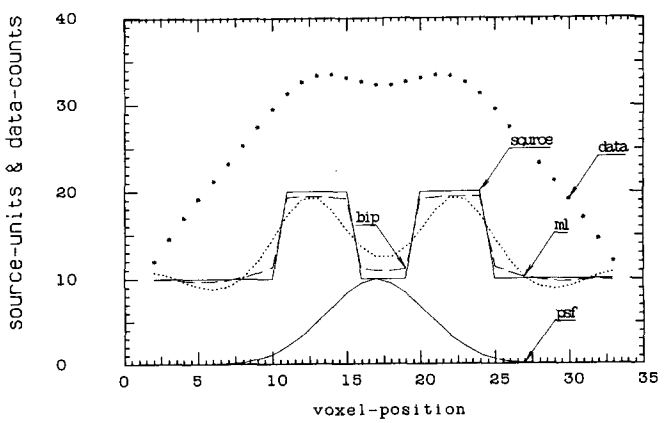

FIG. 3. Results of BIP (broken line) and ML (dotted line) algorithms after 50 and 100 iterations, respectively, with ideal data (stars).

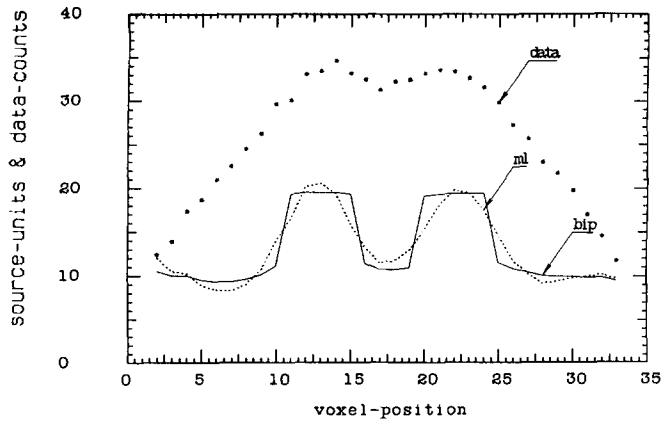

FIG. 4. Comparison of results using BIP (solid line) after 50 iterations and ML (dotted line) after 100 iterations with 2.5% noise Poisson randomized data (stars).

culated from $\Sigma_j R_{ij} S_j$. The Poisson randomized data (stars in Figs. 4 and 5) are obtained from a standard Poisson random number generator.[17]

Figures 1–3 show the results of Bayesian algorithm (BIP, broken line) after 50 iterations and after 100 iterations with the maximum likelihood algorithm (ML, dotted line) [i.e., assuming $P(\Phi)$ is constant in Eq. (5)] for ideal data, where $\phi_b^e \approx 10$, $\phi_s^e \approx 20$ or 30, and $\sigma_l^2 \approx \phi_l^e$. The constants in Eqs. (6) and (9) are chosen as $A \approx 0.05$, $B = N^\tau$, $\tau = 2$, $A_s \approx 15$, $B_s = N^\kappa$, $\kappa = 2$, and N is the number of iterations. The error introduced in the solution due to errors in estimating ϕ_b^e and $\{\phi_s^e\}$ were discussed in Ref. 18.

The corresponding results obtained for Poisson randomized data are shown in Figs. 4–5 for 2.5% and 5% noise,

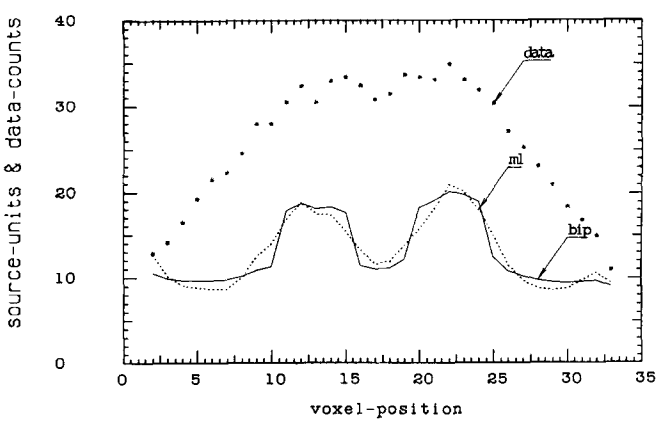

FIG. 5. Results of BIP (solid line) and ML (dotted line) algorithms after 50 and 100 iterations, respectively, with 5% noise Poisson randomized data (stars).

respectively. Improved suppression of boundary Gibbs oscillations is demonstrated and overall improvement in processed images is achieved. With increased noise of $> 5\%$, as expected, image quality is significantly further impaired.

IV. CONCLUSIONS

An *a priori* source probability distribution reflecting a boundary discontinuity and otherwise nearby source element continuity was incorporated into the BIP formalism for image processing in treating measured data obeying Poisson statistics. Improved results were obtained with computer generated ideal and Poisson randomized data, compared to the non-Bayesian maximum likelihood approach.[15,16] Extension of the BIP approach to multidimensional image processing is straightforward.[13] A spectrum of BIP algorithms reflecting different types of *a priori* information [i.e., different $P(\Phi)$'s] is being studied.

[1]T. Huang, *Picture Processing and Digital Filtering* (Springer, NY, 1875).
[2]A. Rosenfeld and A. Kak, *Digital Picture Processing* (Academic, NY, 1982).
[3]B. Friend, "A New Restoring Algorithm for the Preferential Enhancement of Edge Gradients," J. Opt. Soc. Am. **66**, 280 (1976).
[4]E. Hawman, "Image Restoration Subject to Surface Area or Arc Length Constraints," J. Opt. Soc. Am. **67**, 76 (1977).
[5]D. Snyder, M. Miller, L. Thomas, and D. Politte, "Noise and Edge Artifacts in Maximum Likelihood Reconstructions for Emission Tomography," IEEE Trans. Med. Imaging **6**, 228 (1987).
[6]E. Levitan and G. Herman, "A Maximum *a Posteriori* Probability Expectation Maximization Algorithm for Image Reconstruction in Emission Tomography," IEEE Trans. Med. Imaging **6**, 185 (1987).
[7]S. Geman and D. McClure, "Statistical Methods for Tomographic Image Reconstruction," Bull. Iron Steel Inst. London **52**, 38 (1987).
[8]Z. Liang and H. Hart, "Bayesian Image Processing of Data from Generically Constrained Source Distributions," J. Biophys. **49**, 243 (1986).
[9]H. Hart and Z. Liang, "Bayesian Image Processing of Data from Quantitatively Constrained Source Distributions," J. Biophys. **49**, 243 (1986).
[10]Z. Liang and H. Hart, "Bayesian Image Processing of Data from Constrained Source Distributions, I: Non-Valued Uncorrelated and Correlated Constraints," Bull. Math. Biol. **49**, 51 (1987).
[11]H. Hart and Z. Liang, "Bayesian Image Processing of Data from Constrained Source Distributions, II: Valued, Uncorrelated and Correlated Constraints," Bull. Math. Biol. **49**, 75 (1987).
[12]Z. Liang and H. Hart, "Bayesian Image Processing of Data from Constrained Source Distributions–Fuzzy Pattern Constraints," Phys. Med. Biol. **32**, 1481 (1987).
[13]H. Hart and Z. Liang, "Bayesian Image Processing in Two Dimensions," IEEE Trans. Med. Imaging **6**, 201 (1987).
[14]A. Dempster, N. Laird, and D. Rubin, "Maximum Likelihood from Incomplete Data via the EM Algorithm," J. Royal Stat. Soc. **39**, 1 (1977).
[15]L. Shepp and Y. Vardi, "Maximum Likelihood Reconstruction for Emission Tomography," IEEE Trans. Med. Imaging **1**, 113 (1982).
[16]K. Lange and R. Carson, "EM Reconstruction Algorithms for Emission and Transmission Tomography," J. Comput. Assist. Tomogr. **8**, 306 (1984).
[17]B. Carnahan, H. Luther, and J. Wilkes, *Applied Numerical Methods* (Wiley, NY, 1978).
[18]Z. Liang, Ph.D. dissertation, The City University of New York, 1987.